

Thermal evolution of hidden sectors and hidden dark matter

Beyond Standard Model: From Theory to Experiment (BSM-2023)

Hurghada-Egypt

PN

Northeastern University, Boston, Massachusetts, USA.

November 6-9, 2023

BSM physics and hidden sectors

- In exploration of Physics Beyond the Standard Model, hidden sectors play a role in a variety of settings such as in extended supergravity, in strings and in branes, and in moose/quiver theories.
- Much like the visible sector the hidden sector could contain gauge fields and matter fields.
- The success of the electroweak physics in the standard model indicates that the couplings of the hidden sector with the visible sector must be feeble.

- However, how the hidden sector couples with the inflaton is largely unknown.
- The hidden sector could couple with equal strength with the inflaton in which case

$$\xi_0 = \frac{T_h}{T} |_{RH} = 1$$

- Alternately the hidden sector may not couple or has suppressed couplings with the inflaton in which case

$$\xi_0 \simeq 0 |_{TH}$$

- It is of interest to determine how $\xi(T) = T_h/T$ evolves as a function of T since $\xi(T)$ affects relic density, dark matter cross-sections, ΔN_{eff} at BBN, and other observables at low energy.

Recently we have obtained the evolution equation for $\xi \equiv \frac{T_h}{T}$ from energy conservation equations¹.

$$\begin{aligned} \frac{d\rho_v}{dt} + 3H(\rho_v + p_v) &= j_v, \quad (\text{visible sector}), \\ \frac{d\rho_h}{dt} + 3H(\rho_h + p_h) &= j_h, \quad (\text{hidden sector}). \end{aligned}$$

$$\frac{d\xi}{dT} = \left[-\xi \frac{d\rho_h}{dT_h} + \frac{4H\zeta_h\rho_h - j_h}{4H\zeta\rho - 4H\zeta_h\rho_h + j_h} \frac{d\rho_v}{dT} \right] \left(T \frac{d\rho_h}{dT_h} \right)^{-1}.$$

$\zeta = 1$ (radiation dominance), $\zeta = 3/4$ (matter dominance).

Several previous works assume entropy conservation separately for visible and for hidden sectors, i.e., $\frac{s_h}{s_v} = \text{constant}$ which is invalid even for feeble interactions between the visible and hidden sectors.

¹A. Aboubrahim and PN, JHEP **09**, 084 (2022).
 A. Aboubrahim, W. Z. Feng, PN, Wang, Phys.Rev.D 103 (2021) 7, 075014.
 A. Aboubrahim, W. Z. Feng, PN and Z. Y. Wang, JHEP **06**, 086 (2021).

Hidden sector models

- As a concrete example of a hidden sector, we consider a $U(1)_X$ extension of SM with particle content

C_μ : $U(1)_X$ gauge boson; D : (Dirac fermion); ϕ, \mathbf{s} : (spin 0 fields).

- Communication with the visible sector occurs via kinetic ² and Stueckelberg mass mixing ^{3, 4, 5} between the $U(1)_X$ gauge field C_μ and the $U(1)_Y$ hypercharge gauge field B_μ of the SM

(i) Kinetic mixing : $\frac{\delta}{2} C^{\mu\nu} B_{\mu\nu}$,

(ii) Stueckelberg mass mixing : $(m_1 C_\mu + m_2 B_\mu + \partial_\mu \sigma)^2$.

Mass mixing generates a milli-charge on hidden sector matter if such matter is present which is relevant in the explanation of EDGES anomaly ⁶

²B. Holdom, Phys. Lett. B **166**, 196-198 (1986)

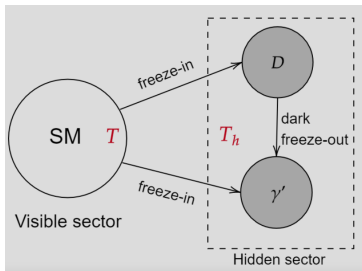
³B. Kors and PN, Phys. Lett. B **586**, 366-372 (2004).

⁴B. Kors and PN, JHEP **12**, 005 (2004).

⁵D. Feldman, Z. Liu and P. N., Phys. Rev. D **75**, 115001 (2007).

⁶A. Aboubrahim, P.N. and Z. Y. Wang, JHEP **12**, 148 (2021).

Hidden and visible sectors in different heat baths



A consistent analysis involves an equation for the thermal evolution function $\xi = T_h/T$.

Dark matter relic density

In this model dark matter is constituted of D -fermions and the computation of the relic density of D involves solutions to yield equations for D and γ' (i are SM fields).

$$\frac{dY_D}{dT} = -\frac{s}{H} \left(\frac{d\rho_v/dT}{4\zeta\rho - 4\zeta_h\rho_h + j_h/H} \right) \left[\langle\sigma v\rangle_{D\bar{D}\rightarrow i\bar{i}}(T)n_D^{eq}(T)^2 - \langle\sigma v\rangle_{D\bar{D}\rightarrow\gamma'\bar{\gamma}'}(T_h)n_D(T_h)^2 + \langle\sigma v\rangle_{\gamma'\bar{\gamma}'\rightarrow D\bar{D}}(T_h)n_{\gamma'}(T_h)^2 \right]. \quad (1)$$

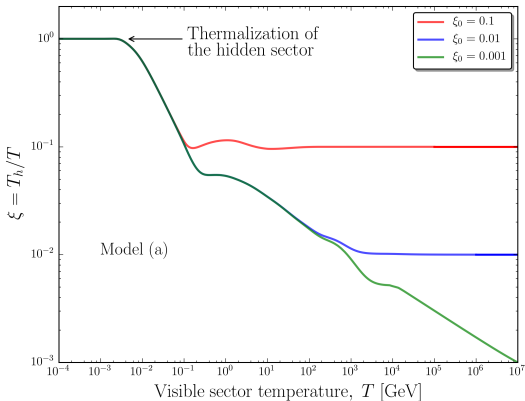
$$\frac{dY_{\gamma'}}{dT} = -\frac{s}{H} \left(\frac{d\rho_v/dT}{4\zeta\rho - 4\zeta_h\rho_h + j_h/H} \right) \left[\langle\sigma v\rangle_{D\bar{D}\rightarrow\gamma'\bar{\gamma}'}(T_h)n_D(T_h)^2 - \langle\sigma v\rangle_{\gamma'\bar{\gamma}'\rightarrow D\bar{D}}(T_h)n_{\gamma'}(T_h)^2 + \langle\sigma v\rangle_{i\bar{i}\rightarrow\gamma'}(T)n_i^{eq}(T)^2 - \langle\Gamma_{\gamma'\rightarrow i\bar{i}}(T_h)\rangle n_{\gamma'}(T_h) \right]. \quad (2)$$

Dark photon is unstable and decays and the entire relic density arises from the dark Dirac fermions D and \bar{D} .

$$\Omega_D h^2 = \frac{s_0 m_D Y_D^0 h^2}{\rho_c}, \quad (3)$$

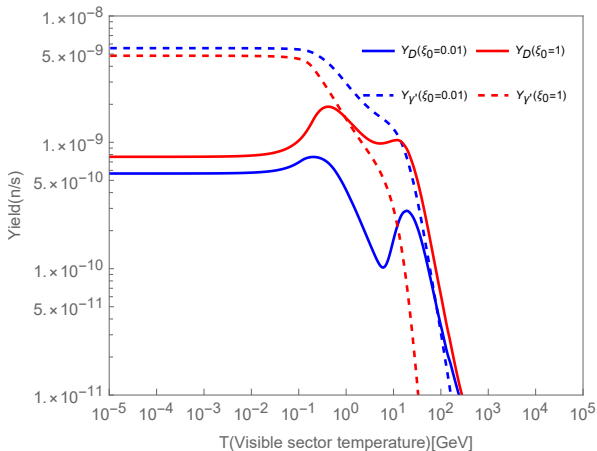
where s_0 is the current entropy density, Y_D^0 which is Y_D at current times.

Solution to yield equations and energy conservation equations exhibit the dependence of $\xi(T)$ on ξ_0 .



The evolution of $\xi(T)$ as a function of T for three different initial values of ξ_0 .

Dark freeze-out for $\xi = 0.01$ vs $\xi = 1$.



Yields of dark fermion (dark matter) and dark photon for $\xi_0 = 0.01$ (blue), and $\xi_0 = 1$ (red). ⁷

⁷J. Li and PN, [arXiv:2304.08454 [hep-ph]] (PRD-to appear)

Dependence of ΔN_{eff} at BBN on ξ_0

- Standard model: $N_{\text{eff}} = 3.046$.
- Planck Collaboration gives $N_{\text{eff}} = 2.99 \pm 0.17$ while the joint BBN analysis of deuterium/helium abundance and the Planck CMB data gives $N_{\text{eff}} = 3.41 \pm 0.45$.
- A conservative constraint is: $\Delta N_{\text{eff}} = N_{\text{eff}}^{\text{exp}} - N_{\text{eff}}^{\text{sm}} \leq 0.25$.
- In the model under discussion, the dark fermion D and dark photon γ' will contribute to the effective neutrino number.

$$\Delta N_{\text{eff}} = \frac{4}{7} g_{\text{eff}}^h \left(\frac{11}{4} \right)^{4/3} \left(\frac{T_h}{T} \right)^4, \quad (4)$$

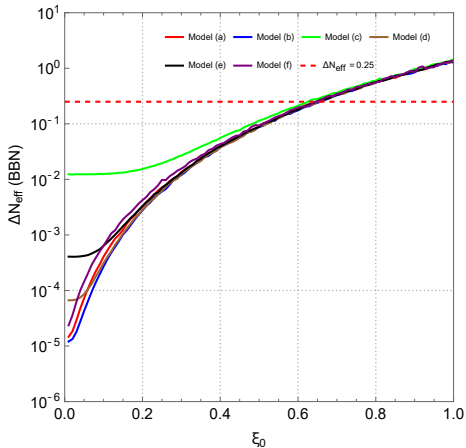
where g_{eff}^h is to be evaluated at the BBN temperature $T_{\text{BBN}} = 1$ MeV.

Dark photon/Dark fermion models consistent with all terrestrial and astrophysical data ⁸

	m_D [GeV]	$m_{\gamma'}$ [MeV]	g_X	δ (in 10^{-9})
(a)	0.354	0.306	0.00738	3.99
(b)	0.259	0.214	0.00675	6.29
(c)	0.281	0.550	0.00931	400
(d)	0.170	0.225	0.00618	19.3
(e)	0.156	0.285	0.00631	52.9
(f)	0.568	0.445	0.00810	2.62

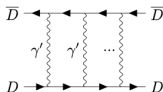
⁸A. Aboubrahim, M. M. Altakach, M. Klasen, PN and Z. Y. Wang, JHEP **03**, 182 (2023) [arXiv:2212.01268 [hep-ph]].

Sensitivity of ΔN_{eff} to ξ_0 ⁹



⁹J. Li and PN [arXiv:2304.08454 [hep-ph]] (to appear in PRD)

Sommerfeld enhancement and ξ_0



$D\bar{D} \rightarrow D\bar{D}$ scattering beyond the Born approximation.

Potential in the non-relativistic limit

$$V(\vec{r}) = \pm \frac{(g_X)^2}{4\pi} \frac{e^{-m_{\gamma'} r}}{r}, \quad (5)$$

where plus for $DD \rightarrow DD$ and $\bar{D}\bar{D} \rightarrow \bar{D}\bar{D}$ and minus for $D\bar{D} \rightarrow D\bar{D}$.
Non-perturbative effects for the process $a + b \rightarrow a + b$ may be written as

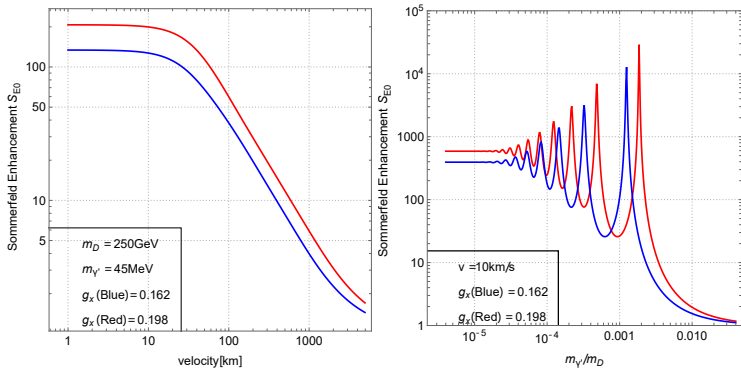
$$(\sigma_{ab} v) = S_E(\sigma_{ab}^0 v). \quad (6)$$

where $(\sigma_{ab}^0 v)$ is the tree level cross section and S_E is the Sommerfeld enhancement.

SE for dark matter cross sections¹⁰

$$\sigma_{DM} = \int d\Omega \left[\frac{d\sigma_{D\bar{D} \rightarrow D\bar{D}}}{d\Omega} + \frac{1}{2} \frac{d\sigma_{DD \rightarrow DD}}{d\Omega} + \frac{1}{2} \frac{d\sigma_{\bar{D}\bar{D} \rightarrow \bar{D}\bar{D}}}{d\Omega} \right], \quad (7)$$

where the factor of $1/2$ arises due to identical nature of particles.



S-wave Sommerfeld enhancement for an **attractive** Yukawa potential for the case $\xi_0 = 0.01$ (blue) and for $\xi_0 = 1$ (red).

¹⁰J. Li and PN [arXiv:2304.08454 [hep-ph]].

Galaxy data indicates velocity dependence of DM cross-sections ^{11, 12}

- Dwarf galaxies:

$$\langle v \rangle \sim (10 - 100) \text{ km/s}$$

$$1 \text{ cm}^2/\text{g} < \frac{\sigma}{m} < 50 \text{ cm}^2/\text{g}.$$

- Midsize galaxies: Milky way, low surface brightness galaxies.

$$\langle v \rangle \sim (80 - 200) \text{ km/s}$$

$$0.5 \text{ cm}^2/\text{g} < \frac{\sigma}{m} < 5 \text{ cm}^2/\text{g}.$$

- Galaxy clusters: Milky way, low surface brightness galaxies.

$$\langle v \rangle > 1000 \text{ km/s}$$

$$0.065 \text{ cm}^2/\text{g} < \frac{\sigma}{m} < 5 \text{ cm}^2/\text{g}.$$

¹¹Tulin, Yu, Phys. Rep.730, 1(2018)

¹²THINGS: The HI (atomic hydrogen) Nearby Galaxy Survey, Fabian Walter et al 2008 AJ 136 2563.

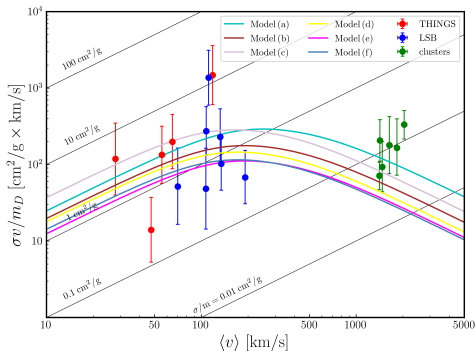
What the galaxy data reveals about nature of dark matter

- Dark matter is collisional at small velocities and collision less at large velocities.
- CDM is collision less and does not have a velocity dependence so CDM does not fit all the data.
- One can explain the data if the cross section behaves like

$$\sigma(v) \propto \frac{1}{v^4}$$

- DM acts like a collisional fluid for small v .
 - It acts like a collision less fluid for large v .
- A model which can produce this behavior is one where the mediator mass is much smaller than the momentum transfer in DM collisions.

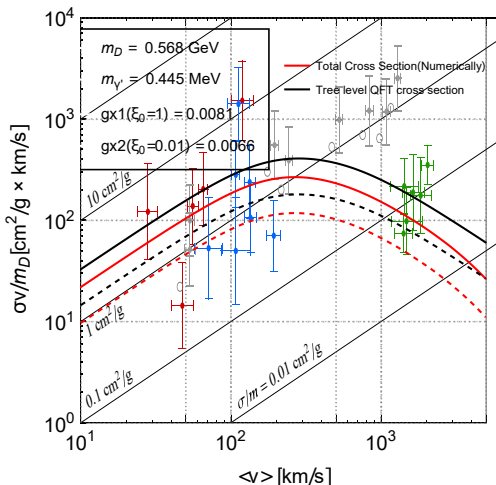
Dark photon model can fit the galaxy from dwarf to galaxy cluster scales ¹³



The fit to the galaxy data indicates the existence of a dark force (the fifth force) arising from dark fermions exchanging hidden dark photons.

¹³Aboubrahim, Feng, PN, Wang, Phys.Rev.D 103 (2021) 7, 075014.

Effect of ξ_0 on galaxy fits



Solid lines are for $\xi_0 = 1$ and the dashed line for $\xi_0 = 0.01$ exhibiting the dependence of $\sigma v / m_D$ on ξ_0 . The fits (in red) are done using the full analysis by numerically integrating the Schrödinger equation including identical particle effects as well as Sommerfeld enhancement. For comparison the tree-level QFT cross section shown by black curves does not consider the effect of identical scattering¹⁴

¹⁴J. Li and P. Nath, [arXiv:2304.08454 [hep-ph]]. (PRD-to appear)

The **approximation** of separate entropy conservation of visible and hidden sectors is **invalid** even for feeble couplings.

In several previous works¹⁵ an assumption of entropy conservation per co-moving volume separately for the visible and the hidden sectors is made to relate $\xi(T)$ at different temperatures, that the ratio s_h/s_v is unchanged, which implies

$$s_v = \frac{2\pi^2}{45} h_{eff}^v T^3, \quad s_h = \frac{2\pi^2}{45} h_{eff}^h T_h^3. \quad (8)$$

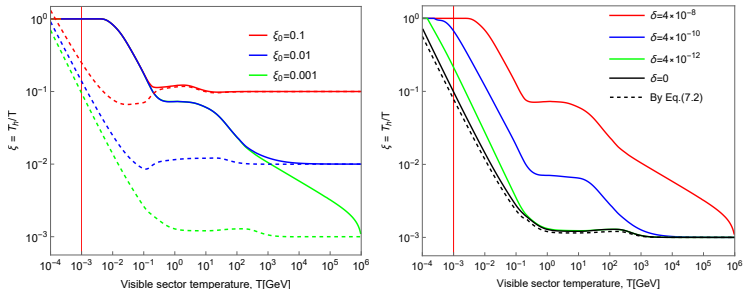
and alternately that the following relation holds

$$\frac{h_{eff}^h(T_h)}{h_{eff}^v(T)} \xi^3(T) = \frac{h_{eff}^h(T_{0h})}{h_{eff}^v(T_0)} \xi^3(T_0) \quad (9)$$

Such an approximation is invalid because of heat exchange between the visible and the hidden sectors even when the couplings between the hidden sector and the visible sectors are feeble.

¹⁵J. L. Feng, H. Tu and H. B. Yu, JCAP **10**, 043 (2008).

An exhibition of lack of validity of separate entropy conservation approximation¹⁶.



$m_D = 2 \text{ GeV}$, $m_{\gamma'} = 2 \text{ MeV}$, $g_X = 0.015$.
Dashed curves: Separate entropy conservation.
Solid curves: Exact analysis.
Left panel: $\delta = 4 \times 10^{-8}$
Right panel: $\xi_0 = 0.001$

¹⁶J. Li and P.N., “Big Bang initial conditions and self-interacting hidden dark matter,” [arXiv:2304.08454 [hep-ph]] (to appear in PRD)

Conclusion

- At the reheat temperature the hidden sector could be very hot ($\xi_0 = \mathbf{1}$) or very cold ($\xi_0 = \mathbf{0}$) or something in between: $\xi_0 = (\mathbf{0}, \mathbf{1})$.
- The formalism presented here gives a synchronous thermal evolution of the hidden and the visible sectors for any given value of ξ_0 .
- The synchronous evolution formalism is of relevance in the development of precision cosmology.
- The approximation of separate entropy conservation in evolution of hidden and visible sectors is invalid even in the case of feeble interactions between the visible and the hidden sectors.